

## FAST TRACK COMMUNICATION

# Interference of spin states in photoemission from Sb/Ag(111) surface alloys

Fabian Meier<sup>1,2</sup>, Vladimir Petrov<sup>3</sup>, Hossein Mirhosseini<sup>4</sup>,  
Luc Patthey<sup>2</sup>, Jürgen Henk<sup>4</sup>, Jürg Osterwalder<sup>1</sup> and J Hugo Dil<sup>1,2</sup>

<sup>1</sup> Physik-Institut, Universität Zürich, Winterthurerstrasse 190, CH-8057 Zürich, Switzerland

<sup>2</sup> Swiss Light Source, Paul Scherrer Institut, CH-5232 Villigen, Switzerland

<sup>3</sup> St Petersburg Polytechnical University, 29 Polytechnicheskaya Street, 195251 St Petersburg, Russia

<sup>4</sup> Max-Planck-Institut für Mikrostrukturphysik, D-06120 Halle (Saale), Germany

E-mail: [jan-hugo.dil@psi.ch](mailto:jan-hugo.dil@psi.ch)


Received 14 December 2010, in final form 28 December 2010

Published 3 February 2011

Online at [stacks.iop.org/JPhysCM/23/072207](http://stacks.iop.org/JPhysCM/23/072207)

## Abstract

Using a three-dimensional spin polarimeter we have gathered evidence for the interference of spin states in photoemission from the surface alloy Sb/Ag(111). This system features a small Rashba-type spin splitting of a size comparable to the momentum broadening of the quasiparticles, thus causing an intrinsic overlap between states with orthogonal spinors. Besides a small spin polarization caused by the spin splitting, we observe a large spin polarization component in the plane normal to the quantization axis of the Rashba effect. Strongly suggestive of coherent spin rotation, this effect is largely independent of the photon energy and photon polarization.

 Online supplementary data available from [stacks.iop.org/JPhysCM/23/072207/mmedia](http://stacks.iop.org/JPhysCM/23/072207/mmedia)

(Some figures in this article are in colour only in the electronic version)

An important branch of spintronics research is looking for new systems with naturally existing spin polarized electrons and ways to manipulate their spins. The broken spatial inversion symmetry at surfaces can induce a spin splitting of electronic states in non-magnetic systems via the spin-orbit interaction. A substantial splitting due to this so-called Rashba effect [1] was observed for the Shockley surface state on Au(111) by angle-resolved photoemission spectroscopy (ARPES) [2]. Later spin resolved experiments confirmed the high degree of spin polarization of the electrons photoemitted from these states [3], observing helical spin structures tangential to the two spin-split Fermi surfaces. More recently, surface alloys of Bi and Pb on Ag(111) have attracted much attention in the search for even larger spin splittings, exploiting a combination of strong atomic spin-orbit interaction of the heavy metals with structural effects enhancing the local potential gradients at the surface [4, 5].

In this communication we discuss the structurally related system of Sb on Ag(111) which has a small but finite spin splitting [6]. The splitting is so small that it cannot be resolved by ARPES in most of the surface Brillouin zone. Nevertheless our spin polarized ARPES data show substantial spin polarization and permit quantification of the spin splitting. More importantly, the measured spin texture is at strong variance with that expected from the Rashba model and suggests that coherent superposition of spin states occur in the photocurrent. We speculate that this effect is also likely to occur in other experimental probes involving electronic excitations, like for example transport measurements.

Spin state interference is an intriguing property of quantum mechanics. For instance, an electron with its spin along the positive  $z$  axis can be represented by two spinors with spins along the  $y$  axis, reading  $\sqrt{2} \cdot \langle z^\uparrow | = (1, 1) = (1, 0) + (0, 1) = \langle y^\uparrow | + \langle y^\downarrow |$ . Similarly, a spin along  $x$  can

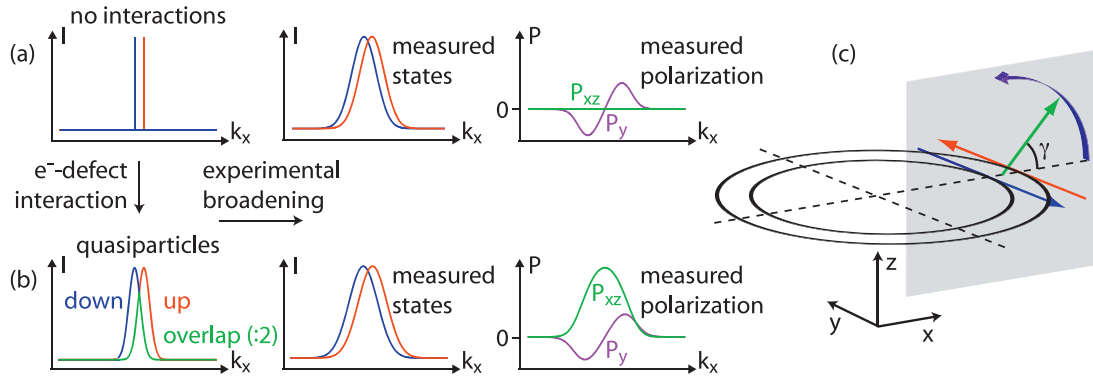


**Figure 1.** Schematic illustration of the suggested mechanism leading to spin polarization in the  $xz$ -plane by spin state interference. A small spin splitting of Rashba-type eigenstates without (a) and with (b) interaction leads, with experimental broadening, to very similar spin integrated data. The resulting polarization spectra are different; for both a Rashba-type spin polarization along the  $y$  direction (violet/dark gray curve) is expected, and for (b) a coherently rotated spin polarization within the  $xz$ -plane (green/light gray curve). (c) Illustration of the associated spin polarization vectors in one region of the spin-split circular Fermi surface.

be written as  $\sqrt{2} \cdot \langle x^\uparrow | = (1, -i) = \langle y^\uparrow | + e^{i3\pi/2} \langle y^\downarrow |$ . A phase difference between  $\langle y^\uparrow |$  and  $\langle y^\downarrow |$  causes a rotation of the resulting spin polarization vector in the  $xz$  plane. As a consequence, the expectation value of the sum of two spinors can differ from the sum of the individual expectation values. In particular, the addition of a spin up and a spin down spinor along some quantization axis does not yield zero polarization, but results in a spinor with an expectation value (henceforth spin polarization) placed within the plane orthogonal to the quantization axis. This is exactly what we observe.

Spin state interference has previously been observed in resonant photoemission induced by circularly polarized light from magnetized Gd by Müller *et al* [7]. In this system, orthogonal spin states can be prepared by the angular momentum transfer from the light and spin-orbit interaction on one hand, and by direct photoemission from magnetized states in the valence band on the other hand. By tuning the photon energy to the 4d resonance, the two spin states can be brought to interfere.

In our case it is the Rashba effect that defines the two orthogonal spin states. Without interactions, but with experimental broadening, the polarization curves will resemble those in figure 1(a). However, these states can interfere when their momentum splitting is of the same order as the intrinsic line width of either state such that they overlap, as illustrated in figure 1(b). The intrinsic line width in photoemission is a consequence of many-body effects of the photohole left behind, which forms, dressed with electron-electron, electron-phonon and electron-defect scattering processes, a quasiparticle [8]. While electron-electron and electron-phonon coupling are inelastic processes, electron-defect scattering is an elastic process and as such preserves the phase relation. In alloy systems, this is expected to be the dominant broadening mechanism. Because the quasiparticles in the overlapping region of the two spin-split bands are indistinguishable in time and space, photoelectrons in this region carry away coherent superpositions in spin space.

Like in the related Bi and Pb surface alloys on Ag(111), the Sb adatoms replace every third Ag atom in the topmost

layer to form a  $(\sqrt{3} \times \sqrt{3})R30^\circ$  superstructure [9, 10], henceforth termed Sb/Ag(111). We also investigated mixed  $Sb_{1-x}Bi_x/Ag(111)$  layers, where Sb is randomly substituted by Bi. In such mixed alloys the spin splitting can be tuned [11, 12], and they can therefore serve as a test for our overlap hypothesis. Finally, we performed photoemission experiments with different photon energies and photon polarization in order to probe the dependence of the spin state interference on these parameters.

The spin polarized ARPES (SARPES) experiments were performed at room temperature at the Swiss Light Source using the COPHEE spectrometer [13]. The energy and angle resolution when measured with the Mott detectors was 80 meV and  $\pm 0.75^\circ$ , respectively. The photoemission setup is schematically shown in figure 2(a). There is a  $45^\circ$  angle between the incoming photons and the detected electrons. The  $z$  axis is given by the sample normal and the sample is rotated around the  $y$  axis. In a momentum distribution curve (MDC) this corresponds to a scan along the  $k_x$  axis with  $k_y = 0$  as shown in figure 2(a) for schematically drawn circular constant energy surfaces. The sample preparation is described elsewhere (see the supporting online material available at [stacks.iop.org/JPhysCM/23/072207/mmedia](http://stacks.iop.org/JPhysCM/23/072207/mmedia)).

In figure 2(b) we show the spin integrated surface state band dispersion of the Sb/Ag(111) surface alloy around the surface Brillouin zone center  $\bar{\Gamma}$  measured along the high symmetry direction  $\bar{\Gamma}\bar{M}$ . Similar to the two related surface alloys Bi/Ag(111) and Pb/Ag(111) [4, 5, 14], two sets of bands are observed. The inner set of bands consists of electrons with a mainly  $sp_z$ -like orbital character while the outer set of bands has a primarily  $p_{xy}$  orbital character. However, the Rashba-type spin splitting is much smaller here and is not resolved in the data of figure 2(b). The smaller splitting can be understood as a consequence of the smaller atomic number  $Z$  of Sb ( $Z = 51$ ) compared to Bi (83) and Pb (82) and a smaller surface corrugation [6, 15, 16].

Bi/Ag(111) and Pb/Ag(111) show Rashba-type spin structures [14], i.e. the spin polarization is mainly in-plane and orthogonal to the electron momentum ( $P_y$  component).

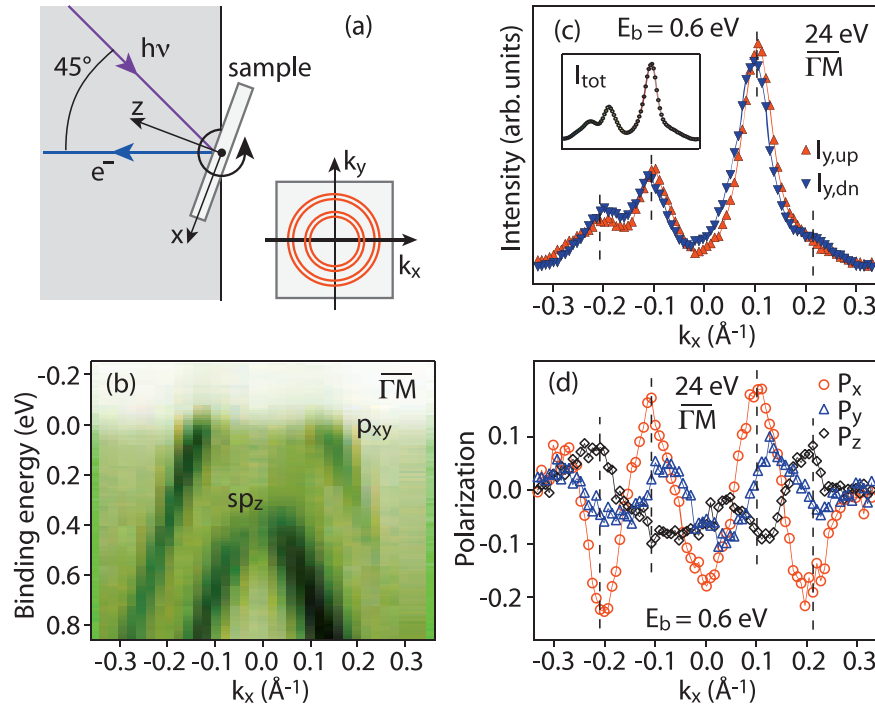


**Figure 2.** (a) Schematic experimental setup. (b) Spin integrated surface state band structure of the Sb/Ag(111) surface alloy around  $\bar{\Gamma}$ . (c) Spin resolved and spin integrated (inset) MDC intensity data for 24 eV photons in the direction  $\bar{\Gamma}\bar{M}$  at  $E_b = 0.6$  eV. (d) Simultaneously obtained spin polarization curves for all three components. The dotted lines are guides to the eye. The momentum region between 0 and  $0.2 \text{ \AA}^{-1}$  corresponds to figure 1.

In figure 2(d) we present spin polarization data obtained for Sb/Ag(111) at a binding energy  $E_b = 0.6$  eV with p-polarized photons of 24 eV (i.e. light polarization in the  $xz$  plane). Here, the spin polarization component  $P_x$  is dominant, corresponding to the radial direction of the constant energy surfaces. It shows large modulation amplitudes centered at the peak positions of the MDCs. This is in sharp contrast to the other systems [17] and represents a major deviation from the Rashba model. The  $P_y$  and  $P_z$  components show modulations with smaller amplitudes, with those in  $P_z$  being rather in antiphase with those in  $P_x$ . On the other hand,  $P_y$  crosses zero at the peak centers, which is typical of Rashba-type behavior [14]. From this latter curve we can produce the spin resolved spectra as projected onto the  $y$  axis [18], which corresponds to the spin quantization axis in the Rashba model (figure 2(c)). The spin resolved MDCs  $I_{y,\text{up}}$  and  $I_{y,\text{dn}}$  show a clear signature of a Rashba-type spin-orbit splitting with a momentum shift  $dk = 2k_0 \cong 0.01 \text{ \AA}^{-1}$  between the two bands (as obtained from fitting the two main peaks).

Another remarkable observation in these data is that the measured spin polarization curves violate time-reversal symmetry. According to this symmetry, the two spin-split partners of the Kramers pairs should have opposite spin polarization vectors for equivalent binding energies, i.e.  $P(k_{\parallel}) = -P(-k_{\parallel})$ . Yet, the polarization curves  $P_x$  and  $P_z$  are symmetric with respect to  $k_x = 0$ . The missing time-reversal symmetry is a strong indication of a photoemission related effect, since time-reversal symmetry has to hold for the initial-state wavefunctions. We suggest that the origin of this photoemission effect is the spin state interference caused by

the coherent part of the intrinsic overlap in each Kramers pair associated with the small spin splitting. Hence similar effects can be expected for other systems with small spin splittings.

The model illustrated in figure 1 can now be directly applied to the case of Sb/Ag(111). Here, the states are split by  $2k_0 \cong 0.01 \text{ \AA}^{-1}$  and the spinor of each state is well defined due to the Rashba effect, termed up and down on the left of figure 1(b). There is a large intrinsic overlap between the two peaks if the momentum broadening is in the order of  $0.01 \text{ \AA}^{-1}$ , which translates to 40 meV energy broadening considering the dispersion. We emphasize again that the phases of the photohole spin states have to be conserved in the many-body interactions, which is the case for momentum broadening due to electron-defect scattering. We were not able to measure the intrinsic line width due to experimental limitations; however for the surface state of the highly perfect Cu(111) surface about 1/3 of the line-width broadening (23 meV) is caused by defects, [19] and for the Al(100) surface state the line-width broadening due to electron-defect scattering is 101 meV [20]. Considering that the Sb/Ag(111) alloy surface certainly has a higher concentration of defects and disorder than the Cu(111) surface due to the nature of the substitutional alloy, [21] it is fair to assume that a significant amount of the broadening is caused by coherent electron-defect scattering. Hence a majority of the photoelectrons in the overlap region represent coherent superpositions of spin up and spin down states.

The peaks can then be divided in regions with purely spin up, purely spin down and an overlap region in order to obtain the scenario shown in figure 1(b). Considering that

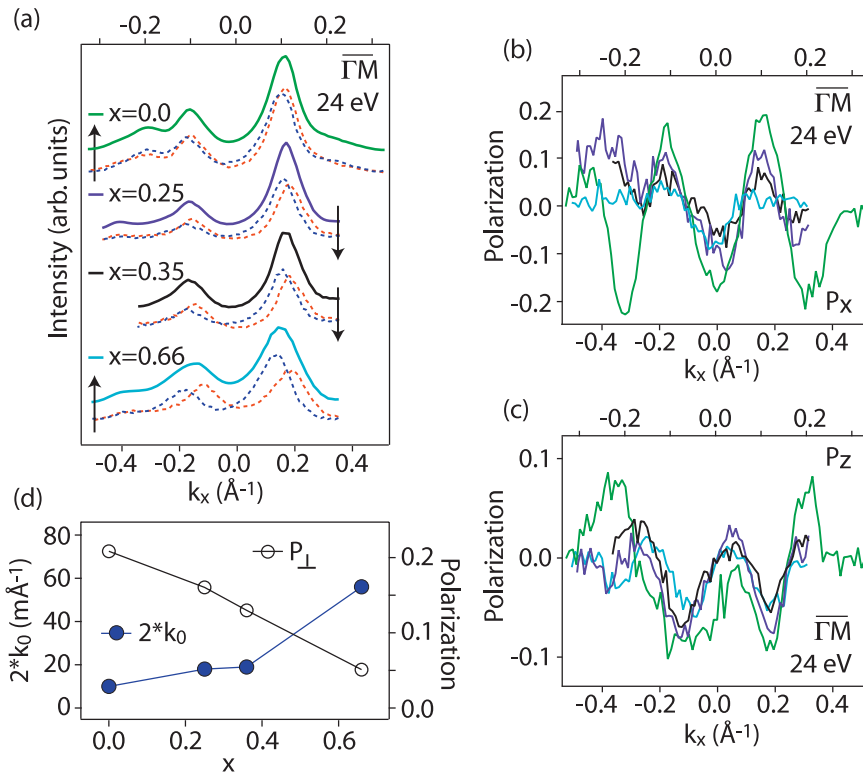


**Figure 3.** (a) Spin integrated MDC data (solid lines) of  $\text{Sb}_{1-x}\text{Bi}_x/\text{Ag}(111)$  for  $x = 0, 0.25, 0.35$  and  $0.66$  at  $E_b = 0.6$  eV ( $x = 0$  and  $0.66$ ) and  $0.9$  eV ( $x = 0.25$  and  $0.35$ ). Dashed lines show the corresponding spin resolved intensity data. For better comparison, the  $k_x$  scale for the  $x = 0$  and  $0.66$  samples is given on the upper side of the frame, while the scale for  $x = 0.25$  and  $0.35$  samples is given on the lower side. The arrows refer to the corresponding  $k_x$  scale. (b), (c) Spin polarization data  $P_x$  and  $P_z$  corresponding to the same samples in (a). Note again the different  $k$ -scales. (d) Spin splitting (full circles) and spin polarization  $P_{\perp}$  (open circles) for different intermixing coefficients  $x$ .

the coherent addition of two orthogonal spinors has a spin polarization vector in the plane normal to the spin polarization of the initial spinors as shown in figure 1(c), spin polarization curves like the rightmost of figure 1(b) are obtained, provided that the relative phases remain constant across the overlap region. In particular, the spin polarization of the overlap region has components  $P_{xz}$  with their maxima at the point of maximum overlap, i.e. centered on the MDC peak. This is exactly what is found in the experiment as shown in figure 2(d). The direction of the spin polarization in the  $xz$  plane, described by the angle  $\gamma$ , is defined by the phase difference between the two orthogonal spin states of the Kramers pair. From the observation that the  $P_x$  and  $P_z$  curves are symmetric with respect to  $k_x = 0 \text{ \AA}^{-1}$  (figure 2(d)), we conclude that corresponding states of opposite  $k_x$  have equal spin rotation angles. For the  $\text{sp}_z$  states we measure  $\gamma = 22^\circ \pm 9^\circ$ , for the  $\text{p}_{xy}$  states the value is  $-25^\circ \pm 10^\circ$ . We can only speculate on which parameters define the phase difference between spin up and spin down states. Likely candidates are the symmetries of initial and final states, and the geometry of the photoemission experiment, i.e. the angle between light incidence and electron detection.

In figure 3 we show SARPES data for  $\text{Sb}_{1-x}\text{Bi}_x$  for  $x = 0, 0.25, 0.35$  and  $0.66$ . From fitting the spin resolved intensity curves  $I_{y,\text{up}}$  and  $I_{y,\text{dn}}$  (red (light gray) and blue (dark gray) dashed lines, respectively) shown in figure 3(a) we find that the spin splitting increases from  $2k_0 = 0.01$  for  $x = 0$  to  $2k_0 =$

$0.056$  for  $x = 0.66$  (figure 3(d)). The amplitudes of the spin polarization curves  $P_x$  and  $P_z$  (figures 3(b) and (c)) decrease markedly as the spin splitting increases. The spin rotation angle in the  $xz$  plane is not strongly affected by the increased spin splitting. Deviations in the rotation angle are within the experimental accuracy. The values  $P_{\perp} = (P_x^2 + P_z^2)^{1/2}$  for the different mixing ratios  $x$  taken at the peak positions are shown in figure 3(d). We thus observe a decrease in the measured spin polarization in the plane normal to the spin quantization axis of the quasiparticles as their splitting gets larger and the intrinsic overlap is reduced. This is fully in line with our model.

Spin polarization observed in photoemission data can have various other origins [22–28], but the outcome depends strongly on the symmetry of the solid and of the particular surface, on photon energy as well as on the absolute directions of photon incidence, photon polarization and electron emission. In order to rule out such effects, we have measured SARPES MDC data for  $\text{Sb}/\text{Ag}(111)$  at a binding energy of  $0.6$  eV for different photon energies and different light polarizations (figure 4). With respect to figure 2, the sample has been rotated by  $90^\circ$  and the MDCs are thus along  $\Gamma\bar{K}$  for figures 4(a)–(f), while (g) and (h) show again a scan along  $\Gamma\bar{M}$ . The upper panels show the MDC intensity data, the lower ones the corresponding spin polarization curves. We observe that the effect is quite robust against variations of these experimental parameters. First, the sample rotation of  $90^\circ$  has no significant influence on the spin polarization

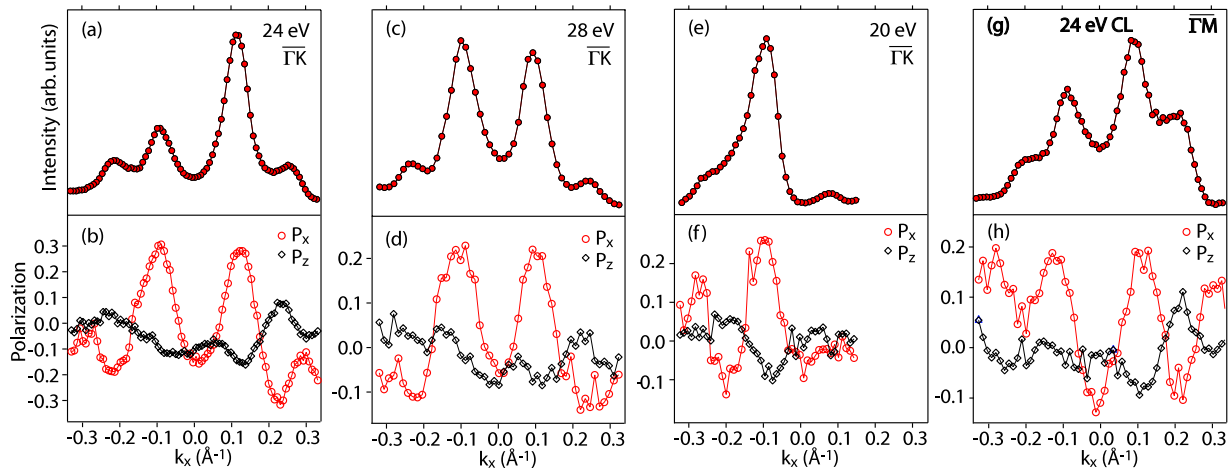


**Figure 4.** SARPES data for Sb/Ag(111) at  $E_b = 0.6$  eV for different photon energies and light polarization. (a), (c), (e) MDC intensity data along  $\Gamma K$  for p-polarized light with photon energies of 24 eV, 28 eV and 20 eV, respectively. (b), (d), (f) Corresponding spin polarization data. (g) MDC intensity data along  $\Gamma M$  for circular left polarized light with  $h\nu = 24$  eV. (h) Spin polarization data corresponding to (g).

curves (figure 2(d) versus 4(b)), in contrast to the effects described by Tamura *et al* [23]. Note that the positions of the outer peaks change slightly due to a hexagonal distortion of their constant energy surface [6]. Second, although the intensity distribution curves change as a function of the photon energy, the spin polarization features are qualitatively not affected. The local extrema for  $P_x$  ( $P_z$ ) are always centered on the peaks, and are positive (negative) for the inner and negative (positive) for the outer ones. The absence of a photon energy dependence (figures 4(b), (d) and (f)) rules out a strong contribution of spin-orbit coupling in the final states to the observed phenomenon. Most striking is the finding that a change from p-polarized to circular left polarized light (figure 2(d) versus 4(h)) has no significant effect on the measured spin polarization curves. Additionally, the spin polarization measured in MDCs is in agreement with the spin polarization measured in energy distribution curves, which excludes changes in the measurement geometry as the cause (see the supporting online material available at [stacks.iop.org/JPhysCM/23/072207/mmedia](http://stacks.iop.org/JPhysCM/23/072207/mmedia)). This corroborates the hypothesis that the measured  $P_x$  and  $P_z$  spin polarization is dominated by the spin structure of the initial states. The experimental spin polarization curves  $P_x$  and  $P_z$  are in disagreement with those obtained by state-of-the-art spin resolved photoemission calculations, which indirectly supports our model of spin interference because the calculations cannot capture coherent effects (see the supporting online material available at [stacks.iop.org/JPhysCM/23/072207/mmedia](http://stacks.iop.org/JPhysCM/23/072207/mmedia)).

Our results should not be confused with the findings of Sakamoto *et al* for the Rashba system Ti/Si(111) [29], where the spin polarization is forced out-of-plane at the  $\bar{K}$  points of the surface Brillouin zone due to a frustration effect. Deviations from pure in-plane ( $P_y$ ) spin polarization can also be caused by local in-plane potential gradients. However, in both cases the states are split and the spins remain paired [4, 14].

Spin state interference has recently been predicted for photoemission from the  $\pi$  states of graphene [30], where

photoelectrons from equivalent atoms within the same unit cell interfere. The authors describe this effect as an interference between spin and pseudo-spin. In contrast, for Sb/Ag(111), the interference stems from a partly coherent intrinsic overlap in  $k$  space.

In summary, we have presented evidence for a coherent superposition of spin states in photoemission from a Rashba system. Interference is assigned to a region in  $k$  space where spin up and spin down states overlap. Hence the measured spin polarization is defined by the photohole quasiparticles and is not significantly modified by final state effects in the photoelectron channel. In condensed matter physics many experiments involve electronic excitations in systems with spin-split states. Similar to the photoemission process described in our work, electron and hole quasiparticles are formed. Specifically, elastic scattering processes should lead to momentum broadening. If this broadening is comparable to the spin splitting, the resulting spin polarization might not behave as expected. Spin state interference may thus be a more general phenomenon.

Fruitful discussions with T Greber, M Hengsberger, M Haverkort, U Heinzmann, B Slomski, C R Ast and I Gierz are gratefully acknowledged. We thank C Hess, F Dubi, and M Klöckner for technical support. This work is supported by the Swiss National Foundation.

## References

- [1] Bychkov Y and Rashba E 1984 *JETP Lett.* **39** 78
- [2] LaShell S *et al* 1996 *Phys. Rev. Lett.* **77** 3419
- [3] Hoesch M *et al* 2004 *Phys. Rev. B* **69** 241401
- [4] Ast C R *et al* 2007 *Phys. Rev. Lett.* **98** 186807
- [5] Pacil  D *et al* 2006 *Phys. Rev. B* **73** 245429
- [6] Moreschini L *et al* 2009 *Phys. Rev. B* **79** 075424
- [7] M ller N *et al* 2006 *Phys. Rev. B* **74** 161401
- [8] Hofmann P *et al* 2009 *New J. Phys.* **11** 125005
- [9] de Vries S *et al* 1998 *Surf. Sci.* **414** 159
- [10] Woodruff D P *et al* 2000 *J. Phys.: Condens. Matter* **12** 7699

- [11] Ast C R *et al* 2008 *Phys. Rev. B* **77** 081407  
[12] Meier F *et al* 2009 *Phys. Rev. B* **79** 241408  
[13] Hoesch M *et al* 2002 *J. Electron Spectrosc. Relat. Phenom.* **124** 263  
[14] Meier F *et al* 2008 *Phys. Rev. B* **77** 165431  
[15] Bihlmayer G *et al* 2007 *Phys. Rev. B* **75** 195414  
[16] Gierz I *et al* 2010 *Phys. Rev. B* **81** 245430  
[17] Dil J H 2009 *J. Phys.: Condens. Matter* **21** 403001  
[18] Meier F *et al* 2009 *New J. Phys.* **11** 125008  
[19] Reinert J *et al* 2004 *Physica B* **351** 229  
[20] Fuglsang Jensen M *et al* 2007 *Phys. Rev.* **75** 153404  
[21] Ast C R *et al* 2007 *Phys. Rev.* **75** 201401  
[22] Henk J *et al* 2004 *J. Phys.: Condens. Matter* **16** 7581  
[23] Tamura E *et al* 1987 *Phys. Rev. Lett.* **59** 934  
[24] Tamura E *et al* 1991 *Europhys. Lett.* **16** 695  
[25] Henk J *et al* 1994 *Europhys. Lett.* **28** 609  
[26] Schmiedeskamp B *et al* 1988 *Phys. Rev. Lett.* **60** 651  
[27] Irmer N *et al* 1992 *Phys. Rev. B* **45** 3849  
[28] Irmer N *et al* 1996 *J. Electron Spectrosc. Relat. Phenom.* **78** 321  
[29] Sakamoto K *et al* 2009 *Phys. Rev. Lett.* **102** 096805  
[30] Kuemmeth F *et al* 2009 *Phys. Rev. B* **80** 241409